Journal of Dentistry xxx (xxxx) xxx

Contents lists available at ScienceDirect

Journal of Dentistry

journal homepage: www.elsevier.com/locate/jdent

Accuracy of single implant scans with a combined healing abutment-scan body system and different intraoral scanners: An in vitro study

Gülce Çakmak [a], Mustafa Borga Donmez [b], Sevda Atalay [c], Hakan Yilmaz [d], Ali Murat Kökat [c], Burak Yilmaz [e,f,g,*]

[a] Buser Foundation Scholar for Implant Dentistry, Department of Reconstructive Dentistry and Gerodontology, School of Dental Medicine, University of Bern, Bern, Switzerland
[b] Department of Prosthodontics, Biruni University Faculty of Dentistry, Istanbul, Turkey
[c] Department of Prosthodontics, Istanbul Okan University Faculty of Dentistry, Istanbul, Turkey
[d] Department of Orthodontics, Yeditepe University Faculty of Dentistry, Istanbul, Turkey
[e] Department of Reconstructive Dentistry and Gerodontology, School of Dental Medicine, University of Bern, Bern, Switzerland
[f] Department of Restorative, Preventive and Pediatric Dentistry, School of Dental Medicine, University of Bern, Bern, Switzerland
[g] Division of Restorative and Prosthetic Dentistry, The Ohio State University College of Dentistry, OH, USA

ARTICLE INFO

Keywords:
Accuracy
Healing abutment-scan body
Intraoral scanner
Precision
Trueness

ABSTRACT

Objective: The aim of the present study was to evaluate the accuracy of single implant scans with a combined healing abutment-scan body (CHA-SB) system using different intraoral scanners.
Methods: A partially edentulous model with an implant was fabricated, and a CHA-SB system was secured on the implant. The model was scanned using an industrial-grade blue light scanner (ATOS Core 80) and a master reference model was generated (MRM). The model was also scanned with 4 different intraoral scanners (IOSs) [(Virtuo Vivo (VV), TRIOS 3 (T3), Omnicam (CO), and Primescan (PS)]. Test scans (n = 8) were superimposed over the MRM using the best fit algorithm (GOM Inspect 2018; GOM GmbH). After superimpositions, distance and angular deviations at selected areas on CHA-SB system were calculated. The data were analyzed with a 1-way ANOVA and Tukey HSD tests for trueness and precision (α=0.05).
Results: The differences in trueness (distance deviations) among tested IOSs were nonsignificant (P=.652). VV presented the highest angular deviations ($P \leq$.031), and the angular deviations in other IOS scans were not found different ($P \geq$.378). The precision of distance deviation data was not significantly different among scanners (P=.052). For the precision of angular deviation data, significant differences were found among IOSs (P=.002). Compared with PS (P=.007) and T3 (P=.014), VV had significantly lower precision, which was not significantly different than that of CO (P=.815).
Conclusions: The accuracy (angular deviation) of scans of a combined healing abutment-scan body system on a single implant varied depending on the IOS. VirtuoVivo scans had the lowest accuracy in terms of angular deviations. When the distance deviation data were considered, scan accuracy of scanners was similar.
Clinical Significance: A recently introduced combined healing abutment-scan body system combines the acquisition of both the implant and the soft tissue. When different intraoral scanners scan the combined healing abutment-scan body system, the scan accuracy may vary.

1. Introduction

Impression of a dental implant can be taken digitally with scanners (intraoral or laboratory) and the scans can be processed by using computer aided design-computer aided manufacturing (CAD-CAM) technologies [1-3]. Digital workflow consists of two methods, direct or indirect [3-5]. With the indirect method, a stone cast, which is obtained after a conventional impression, is digitized with a laboratory scanner (LBS) and scan bodies [3, 4, 6]. Direct workflow includes intraoral scanners (IOSs) and scan bodies (ISBs) [6], and has certain advantages over indirect method as the intraoral data is directly transferred to the laboratory, and potential conventional impression- and stone

* Corresponding author.
E-mail address: burak.yilmaz@zmk.unibe.ch (B. Yilmaz).

https://doi.org/10.1016/j.jdent.2021.103773
Received 30 April 2021; Received in revised form 28 July 2021; Accepted 3 August 2021
Available online 9 August 2021

cast-related flaws are eliminated [2, 7, 8]. Regardless of the technique, the CAD starts with the replacement of the SB's scan, which is an approximation of the real SB, with the corresponding library file that is available in the CAD system. However, problems may arise if the congruence between the library file and the SB's scan is not optimal [9].

ISBs are available in different shapes and sizes and most ISBs are cylindrical or conical, which, in some situations, doesn't enable proper soft tissue contouring for an optimal emergence profile. In addition, with apically placed implants, removal of the HA may traumatize the soft tissues, and accurate positioning of the ISB may be challenging due to the thickness of the soft tissues around the platform (neck) of the implant [3].

Coded healing abutments (HAs) were first introduced in 2004 to be used with conventional impression techniques [10]. Then, the coded HAs became available for digital implant scans [11] as the data regarding the position, type, and size of the implant are embedded in their occlusal surface codes [6, 10, 12]. Coded HAs can be scanned after the soft tissues are healed or the scan can be performed immediately after implant placement or uncovering, which avoids the need for a separate scan appointment [13]. Therefore, the placement of the definitive crown is facilitated. Avoiding a separate scan appointment minimizes the peri-implant soft tissue irritation as the number of times the HA is removed and tightened back on the implant is reduced [12]. Recently, a combined healing abutment-scan body (CHA-SB) system, which consists of a contoured HA and an ISB, has been introduced [13, 14]. CHA-SB system enables contouring of soft tissues for a proper emergence profile, which helps the soft tissues to better tolerate the placement of a definitive restoration at the delivery appointment. The implant and the soft tissue can be scanned at once as the contoured emergence profile of the HA already exists in the software, enabling its reproduction on the definitive restoration.

Accuracy can be described as the proximity to the actual dimensions of an object and it is the combination of trueness and precision [2, 7, 15]. Trueness is defined as the closeness of the measurement to the real sizes of an object, whereas precision is described as the closeness of repeated measurements of an object to each other. High trueness means a close result to the measured object, as high precision is achieved through predictable and repeatable measurements [16]. Current LBSs and IOSs use varying mechanisms to capture the raw data in point cloud form [2, 4, 17], and the use of IOSs with different scan mechanisms may result in differences in accuracy [18]. IOS-ISB interaction may also affect the scan accuracy due to the differences in scan mechanisms [3, 4]. The use of CHA-SB has been reported in a clinical report [15], however, studies on the scan accuracy when CHA-SB is used are lacking [19]. No studies yet compared the scan accuracy when the CHA-SB system is digitized with different IOSs. Therefore, the purpose of this study was to compare the accuracy (trueness and precision) of single implant scans of the CHA-SB system when 4 different IOSs with different data acquisition technologies were used. The null hypotheses were that i) IOSs would not affect the trueness and ii) IOSs would not affect the precision of the single implant scans when the CHA-SB system is scanned.

2. Materials and methods

A poly(methyl methacrylate) (PMMA) mandibular partially edentulous master model was fabricated with a single implant at the first molar site (4.0 mm × 11 mm, Neoss ProActive Straight, Neoss Implant System, Harrogate, England). Implant was placed positioning its inner slot (groove) buccally to align the indexed HA in this slot according to the manufacturer's recommendations [13, 14].

A polyetheretherketone (PEEK) HA (Esthetic Healing Abutment, Neoss Implant System, Harrogate, England) of the CHA-SB system (Fig. 1) was tightened to the implant with a screw driver lining up with the buccal groove in the implant. The groove enables correct positioning of the anatomic shape of the HA, and the position of the implant can be acquired when the CHA-SB is scanned. Then, a medical grade acrylic

Fig. 1. Combined healing abutment (left) and scan body (right) system (separated parts at the top and when combined at the bottom).

resin SB (ScanPeg, Neoss Implant System, Harrogate, England) was inserted into the HA. When positioning the SB into the HA, a vertical outdent on the SB was aligned with an indent (keyway) in the HA (Fig. 2) [13, 14]. The SB is secured in the HA through friction. The HA-SB connection enables one certain SB position in the HA horizontally, and the indent-outdent prevents the rotation of the SB [13]. This connection is different than a conventional SB-implant connection, where the SB is secured in the implant with a screw. The components of the CHA-SB system were not separated until all scans were completed.

Before scanning, a 2 μm thin layer of antireflective powder was sprayed on the surface of the master model. A master reference model standard tessellation language file (MRM-STL) was created by scanning the model with an industrial-grade blue light scanner (ATOS Core 80 5MP, GOM GmbH, Braunschweig, Germany), which has a 6 μm sphere space error and 8 μm size error, and then reverse engineered via a digitizing software (Pro 8.1, GOM GmbH, Braunschweig, Germany) [2].

Four different IOSs with different scan mechanisms were used to acquire the scans: TRIOS 3 (T3) (Cart version 1.4.7.5, 3Shape, Copenhagen, Denmark) utilizes confocal microscopy and ultrafast optical scanning technology, Cerec Omnicam (CO) (version 4.6.1, Cerec-Dentsply Sirona, Bensheim, Germany) depends on optical

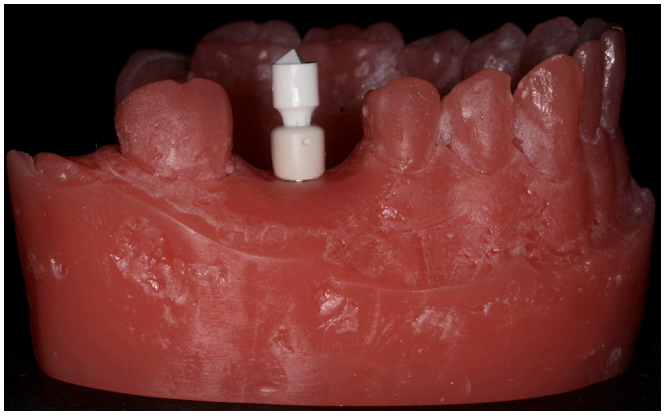

Fig. 2. Poly(methyl methacrylate) (PMMA) master model.

triangulation and confocal microscopy, Cerec Primescan (PS) (version 5.0.0, Cerec-Dentsply Sirona, Bensheim, Germany) uses smart pixel sensor, and Virtuo Vivo (VV) (version 3.0, Dentalwings, Montreal, Quebec, Canada) operates on a blue laser scanner with multiscan imaging technology. Eight consecutive scans were made with each IOS by the same operator in a humidity and temperature controlled room (G. Ç.). Calibrations were performed by the same operator before each scan and all scans were completed with following the recommendations IOS manufacturers. All scans started from the molar distal to the implant. Scan strategies used in the present study were as follows:

CO: The scan started capturing half of the arch from the occlusal aspect of the molar and scanned the lingual surfaces to the lateral incisor on the other side of the arch. Then, occlusal surfaces were scanned moving back distally to the starting point. Half-arch scan was completed by scanning the buccal surfaces. This scanning sequence was also implemented for the acquisition of the opposite quadrant [20].

PS: Scan started capturing the lingual surfaces, and then the occlusal surfaces in the entire arch were scanned moving back to the starting point, and the acquisition was completed by scanning the buccal aspects [21].

T3: The scan was started from the occlusal surface and captured the entire arch, with a return to scan the lingual surfaces as recommended by the manufacturer. Acquisition was completed by scanning the buccal surfaces [22].

VV: This IOS had no recommended strategy defined by the manufacturer, therefore, the scan path of T3 was adopted.

Once all SB and master model surfaces were captured without any major imperfections, a scan was considered complete [1].

To evaluate the accuracy, IOS scans (test scans) were converted to STL files and superimposed over the MRM-STL (nominal scan) with a three-dimensional (3D) metrology software (GOM Inspect 2018, GOM GmbH, Braunschweig, Germany) by using the best fit algorithm [2]. Nominal and test scans (IOS scans) were superimposed with the prealignment feature of the software for initial alignment followed by using the "Local best-fit" feature of the software to minimize errors.

In order to determine the trueness (distance and angular deviations) of IOS scans, a coordinate system was created [2] and the mean distance and angular deviations were calculated for each IOS. A circular plane was created on the uppermost surfaces of the SBs in nominal and test scans [2]. One additional circle for each of the scans (one for nominal and 1 for each IOS test scan) 3 mm below and parallel to the top circular plane was generated (Fig. 3). The linear deviations between the two circles on each scan were then calculated in x, y, and z axes. The 3D distance deviations in each IOS scan were calculated by using the following formula: $3D=(\sqrt{x^2+y^2+z^2})$ [2].

Angular deviations were measured by using the same software, by calculating the angle between the circles (both in nominal and IOS test scans). Nominal was accepted as 0-out one position and the 3D angle in between these circles was recorded [2].

The congruence between the MRM-STL and the library file of the CHA-SB was also evaluated by using the abovementioned methods to verify the fit between the HA and the SB (Fig. 4).

The statistical evaluation of the results was performed (IBM SPSS Statics 25.0, SPSS Inc, Chicago, IL). Means and 95% confidence limits for distance and angular deviation data were calculated. The data obtained were compared with 1-way analysis of variance (ANOVA), and the Tukey HSD Post-Hoc analysis was utilized to resolve significant interactions (α=0.05). The number of scans for each IOS was determined by a power analysis (power: 0.80, α: 0.05, and effect size: 0.6) based on the results of a previous study [2]. After the initial analysis, it was observed that the sample size allowed the detection of highly statistically significant differences; therefore, no additional scans was deemed necessary. The homogeneity of the variances among scanners was evaluated for precision [2, 4] by using the Student's *t*-test ($\alpha = 0.05$).

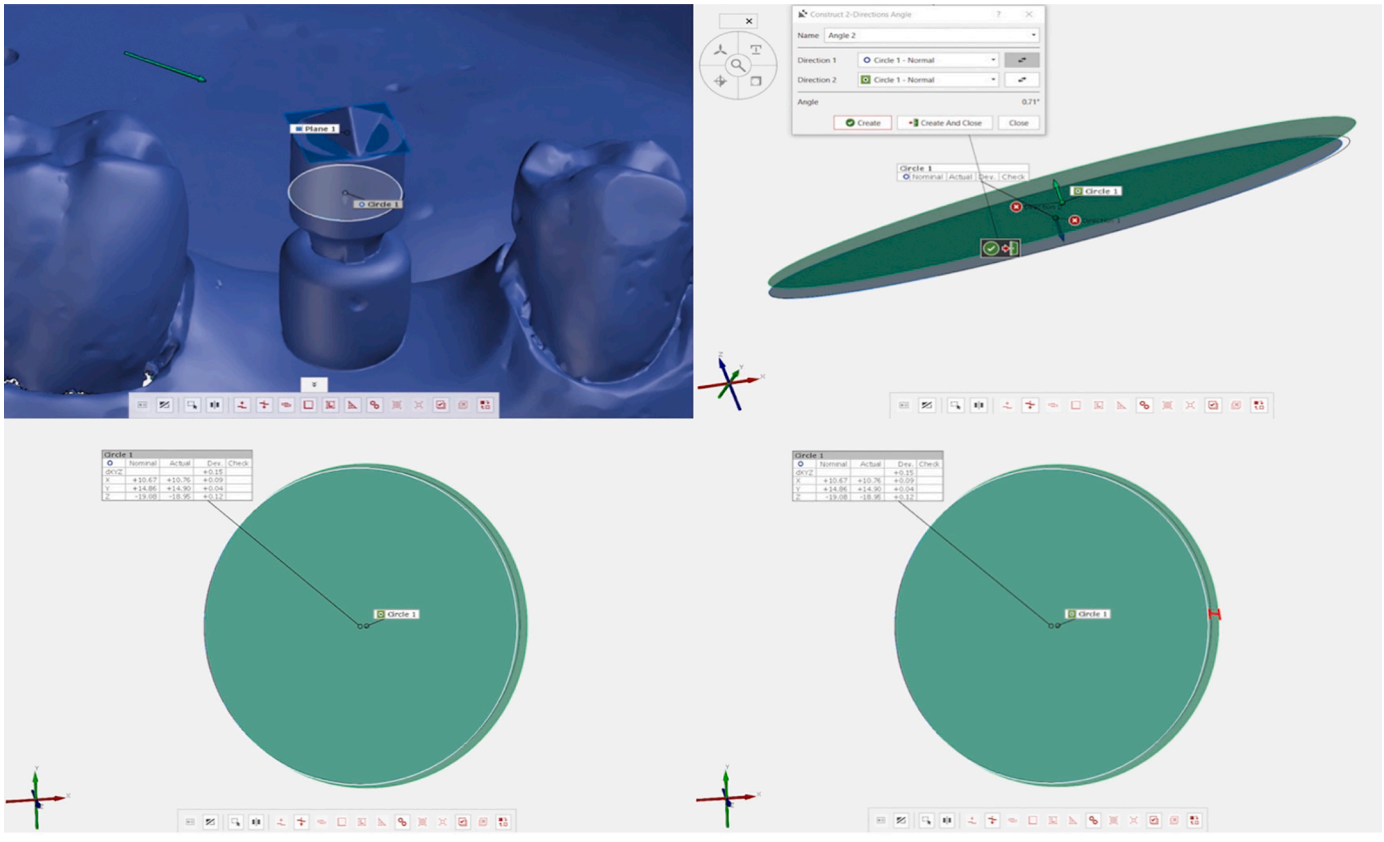

Fig. 3. Circular planes generated for the distance and angular deviation measurements.

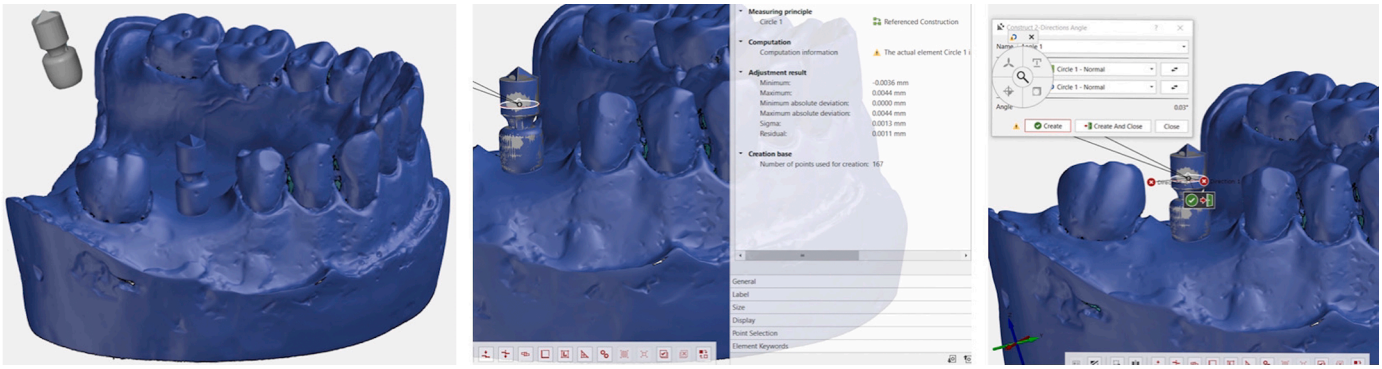

Fig. 4. The congruence between the MRM-STL and the library file of CHA-SB.

3. Results

The superimposition of the MRM-STL over the library CAD file of the CHA-SB system revealed a maximum linear deviation of 4.4 μm and an angular deviation of 0.03° (Fig. 4).

The results of the Tukey HSD test are presented in Table 1. One-way ANOVA results of the trueness revealed that the IOS had a significant effect on angular deviations ($F = 0.551$, df=3, and P=.001). VV had the highest mean angular deviations (P=.031 vs CO, P<.0001 vs T3, and P=.006 vs PS). The mean angular deviation with VV was 1.25±0.63° and the estimated difference in means was 0.66 with CO, 1.03 with T3, and 0.81° with PS. However, angular deviations compared with the other tested IOSs were not significantly different ($P \geq .378$). IOS's effect on distance deviations was nonsignificant (P=.652).

One-way ANOVA revealed that the IOS had a significant effect on precision of the scans (angular deviation data) ($F = 6.227$, df=3, and P=.002). VV had significantly lower precision (angular deviation data) compared with PS (P=.007) and T3 (P=.014). Difference in precision between VV and CO (P=.815), and PS and T3 (P=.992) was not significant. For precision of distance deviation data, no statistical difference was found among IOSs ($F = 2.908$, df=3, and P=.052).

4. Discussion

The first null hypothesis that the trueness (3D distance and angular deviations) would not be affected by the IOS type was rejected as angular deviations varied in the scans of different IOSs. The second null hypothesis was also rejected as the scan precision of IOSs was different in terms of angular deviation data. Precision of CO (distance deviation data) was lower than that of other IOSs, but, this finding should be interpreted cautiously as the P value was only slightly above 0.05 (P=.052).

In the present study, the trueness and precision of distance deviation data in different IOS scans were similar, but, the trueness and the precision of angular deviation data showed significant differences amongst the scans of IOSs. VV presented the lowest trueness and had lower precision (angular deviation data) along with CO, compared with the other two IOSs. Accordingly, VV had the lowest accuracy among the IOSs tested, which use varying data acquisition technologies [2, 8, 23] that may be the reason for the differences in their accuracy. Nevertheless, all tested IOSs in the present study presented lower distance deviations than 150 μm (Table 1), which may be considered clinically acceptable [24]. The distance deviation results in the present study are also within the range of previous studies for single implant scans, which was 22.3 to 226.23 μm [7, 23] for T3, from 28.4 to 372.48 μm [7, 23] for CO, and from 43.35 to 204.4 μm [23] for PS. The distance deviation values reported for VV ranged from 38 to 79 μm [2, 8] when multiple implants were scanned. The studies on the accuracy of IOSs tested in the present study are generally based on multiple-implant scans [2, 8, 25, 26]. Since VV is a recently introduced IOS [2], not many studies have investigated its performance, and future studies are necessary to report its deviation range and to broaden the knowledge on the performance of other IOSs when a single implant is scanned.

Table 1
Mean distance (μm) and angular deviation (°) values for different IOSs.

IOS	Distance Deviation (μm) for Trueness	Angular Deviation (°) for Trueness	Distance Deviation (μm) for Precision	Angular Deviation (°) for Precision
VV	105.3 ± 26.5^{a}	1.25 ± 0.63 ^{b}	18.8 ± 17.2^{a}	0.53 ± 0.28^{b}
T3	127 ± 21.2^{a}	0.22 ± 0.15 ^{a}	14.1 ± 14.9^{a}	0.12 ± 0.09^{a}
CO	124.6 ± 58.6^{a}	0.59 ± 0.61 ^{a}	47.5 ± 29.4^{a}	0.42 ± 0.41^{ab}
PS	126.6 ± 41.4^{a}	0.44 ± 0.11 ^{a}	24.6 ± 32^{a}	0.08 ± 0.07^{a}

Different superscript lowercase letters in same column indicate significant differences among groups (P<.05).

An inaccurate scan may lead to an ill-fitting definitive prosthesis [8], and a recent review on the effect of IOSs on the marginal accuracy of CAD-CAM crowns reported the significance of the IOS type [27]. Higher distance and angular deviations may also affect the interproximal and occlusal contacts of definitive restorations, and authors are unaware of a study, which evaluated the proximal or occlusal contact of the restorations fabricated by using the scans of different IOSs. Taking into account that VV had scans with lower accuracy (angular deviations), definitive restorations fabricated with the scans of VV may require more intraoral/chairside adjustments.

In a previous study [8], where the trueness was compared among 12 IOSs when scanning an edentulous maxilla with 6 implants, CO had the lowest trueness among the IOSs tested in the present study when mesh/mesh method (superimposing the virtual models obtained with IOSs with a reference model derived from a certified scanner) was used. In another study [7], the accuracy of 5 IOSs was evaluated for the scans of a single implant, two implants to be restored with a partial prosthesis, or a complete maxillary arch with 6 implants. T3 had higher scan accuracy for the single implant scan compared with CO. Similarly, in the study by Imburgia et al. [25], T3 had higher trueness than CO when a partially edentulous maxilla (3 implants) was scanned, and no significant difference in precision was reported. The accuracy of T3 and CO was similar when an edentulous maxilla was scanned. The trueness of the scans of 10 IOSs using a simulated implant SB in a partially edentulous mandibular model was evaluated in another study, and PS and T3 presented better trueness than CO [23]. In the present study, the accuracy of T3, CO, and PS was similar. Nevertheless, direct comparison of the results of the present study with abovementioned studies [7, 8, 23, 25] is not possible, since the SB design in those studies was different than that of CHA-SB.

Previous studies that investigated the accuracy of scans widely used conventional SBs, which were tightened directly on implants [1, 2, 4, 6]. However, SB in CHA-SB system is secured on an HA and the connection between the HA and the SB does not involve a screw; the fit between the HA and the SB is through friction. Clinician should make sure that the SB

seats in the HA completely by pressing on the SB, and the antirotational feature provides horizontal stability. Nevertheless, conventional SBs may also present with seating issues particularly when the implant is placed deep apically, an implant with a deeply tapered internal connection is used, and a mismatch is present between the base of the SB and the internal connection of the implant [3]. Considering that the HA and SB assembly's interface is supragingival, it may be easier to detect potential seating errors due to high visibility of the area. The fit between the HA and the SB in the present study was assessed by evaluating the congruence between the MRM-STL file with the corresponding library file. To the authors' knowledge, only one study has evaluated the congruence between the meshes of SBs and the library CAD file [9]. Mangano et al. [9] reported deviation values ranging from 25.5 to 38.3 μm, which are higher than the calculated deviation from the library file in the present study. The favorable congruence found in the present study may be an indicator of the easy insertion of the SB into the HA. The congruence between the meshes and the library file was reported to be affected by the type of the scanner [9]. The present study evaluated the congruence between the master model mesh and the library file to assess the assembly between the HA and the SB. Future studies should evaluate the reliability of the CHA-SB scans performed with different IOSs evaluating the congruence between the intraoral scanners' scans and the library file. The findings of such a study may enable improved understanding of potential clinical outcomes with the tested system.

The accuracy of SBs may be affected by the manufacturing tolerances [28, 29] as various types of materials (titanium alloys, PEEK, aluminum alloy, and resins) are used for the body part of the SBs [3]. Schmidt et al. [28] investigated the manufacturing tolerance of three ISBs by using x-ray computed tomography and concluded that manufacturing tolerances had the potential to affect the accuracy. A recent study substantiated these findings; the authors reported tolerances in height, diameter, and plane measurements of 6 different 1-piece SBs and the height measurements in conical connection implants had the highest tolerances and deviations [29]. Considering that the CHA-SB is a 2-piece system, the manufacturing tolerance might have a greater effect on the scan accuracy compared with a 1-piece SB. The effect of manufacturing tolerance on CHA-SB system's scan accuracy should be investigated in future studies.

A recent study compared the scan accuracy when the CHA-SB system was used with direct workflow and a conventional SB was used with direct or indirect workflows. All tested workflows presented similar accuracy [19]. Yılmaz et al's [21] study used one of the IOSs investigated in the present study (TRIOS 3) to scan the CHA-SB system and the deviation values ranged between 50 and 178 μm, which are in line with the deviations found in the present study.

Previous publications on ISBs concluded that the interaction between the ISB design and the scanner technology is crucial for digital scans [3, 4]. In addition, the IOS's scan accuracy evaluation may be affected by the reference scanner, choice of the digitization method, best-fit alignment, and distribution and number of surface data points [6]. The reference scanner used in the present study is a high-accuracy industrial structured-light scanner. This scanner and the metrology software program used in the present study have been commonly used in dental research studies for accuracy measurements [2, 30]. The standardization and accuracy of deviation calculations in the present study were attempted to be optimized with the use of these 2 metrology-grade digital research tools.

The present in vitro study was performed under standardized conditions, however, scan accuracy may be influenced by patient specific factors, the environment the scans were performed, and the presence of saliva or blood [1, 4, 8]. One experienced operator performed the scans, however, operator experience might affect the accuracy of intraoral scans [26, 31, 32]. Thus, the findings may vary depending on the operator. The scan accuracy may be affected by the number of implants, [7, 25], therefore, the CHA-SB system should be scanned when used on multiple implants to evaluate the effect of number of implants on the scan accuracy. The CHA-SB can only be used with a certain implant brand, which limits its applicability [13]. The CHA-SB is a relatively new system and to the authors' knowledge, the present study is the first study that evaluated the effect of IOS on the scan accuracy. Nevertheless, clinical studies are necessary to corroborate the findings of the present in vitro study and to better understand the clinical outcomes. Future studies should also investigate the effects of different IOSs on the accuracy of definitive restorations fabricated by using the CHA-SB scans.

5. Conclusions

The following conclusions were drawn according to the findings of this in vitro study:

1 The accuracy (trueness and precision) of single implant scans of combined healing abutment-scan body system was similar with tested IOSs in terms of distance deviations.
2 The accuracy of scans of combined healing abutment-scan body system for angular deviations was significantly different among tested IOS. VirtuoVivo presented the lowest accuracy for angular deviation data.

Author contribution statement

Gülce Çakmak: Design, Data collection, Drafting article, Critical revision of article

Mustafa Borga Donmez: Drafting article, Critical revision of article

Sevda Atalay: Design, Data collection, Drafting article

Hakan Yilmaz: Data analysis, Data interpretation, Statistical analysis.

Ali Murat Kökat: Design, Critical revision of article

Burak Yilmaz: Data interpretation, Critical revision of the article, Approval of the submitted and final versions

Declaration of Competing Interest

The authors declare that they have no known competing financial interests or personal relationships that could have appeared to influence the work reported in this paper.

Acknowledgments

Neoss Implant System is gratefully acknowledged for supplying the materials used in this study. The authors also thank Gökhan Akcagöz for supplying the materials.

References

[1] R.M. Mizumoto, G. Alp, M. Özcan, B. Yilmaz, The effect of scanning the palate and scan body position on the accuracy of complete-arch implant scans, Clin. Implant. Dent. Relat. Res. 21 (2019) 987–994, https://doi.org/10.1111/cid.12821.
[2] G. Çakmak, H. Yilmaz, A. Treviño, A.M. Kökat, B. Yilmaz, The effect of scanner type and scan body position on the accuracy of complete-arch digital implant scans, Clin. Implant. Dent. Relat. Res. 22 (2020) 533–541, https://doi.org/10.1111/cid.12919.
[3] R.M. Mizumoto, B. Yilmaz, Intraoral scan bodies in implant dentistry: a systematic review, J. Prosthet. Dent. 120 (2018) 343–352, https://doi.org/10.1016/j.prosdent.2017.10.029.
[4] R.M. Mizumoto, B. Yilmaz, E.A. McGlumphy Jr., J. Seidt, W.M. Johnston, Accuracy of different digital scanning techniques and scan bodies for complete-arch implant-supported prostheses, J. Prosthet. Dent. 123 (2020) 96–104, https://doi.org/10.1016/j.prosdent.(2019).01.003.
[5] H. Rudolph, H. Salmen, M. Moldan, K. Kuhn, V. Sichwardt, B. Wöstmann, R. G. Luthardt, Accuracy of intraoral and extraoral digital data acquisition for dental restorations, J. Appl. Oral. Sci. 24 (2016) 85–94, https://doi.org/10.1590/1678-775720150266.
[6] B. Batak, B. Yilmaz, K. Shah, R. Rathi, M. Schimmel, L. Lang, Effect of coded healing abutment height and position on the trueness of digital intraoral implant scans, J. Prosthet. Dent. 123 (2020) 466–472, https://doi.org/10.1016/j.prosdent.(2019).06.012.

[7] F.G. Mangano, U. Hauschild, G. Veronesi, M. Imburgia, C. Mangano, O. Admakin, Trueness and precision of 5 intraoral scanners in the impressions of single and multiple implants: a comparative in vitro study, BMC Oral Health 19 (2019) 101, https://doi.org/10.1186/s12903-019-0792-7.

[8] F.G. Mangano, O. Admakin, M. Bonacina, H. Lerner, V. Rutkunas, C. Mangano, Trueness of 12 intraoral scanners in the full-arch implant impression: a comparative in vitro study, BMC Oral Health 20 (2020) 263, https://doi.org/10.1186/s12903-020-01254-9.

[9] F. Mangano, H. Lerner, B. Margiani, I. Solop, N. Latuta, O. Admakin, Congruence between meshes and library files of implant scanbodies: an in vitro study comparing five intraoral scanners, J. Clin. Med. 9 (2020) 2174, https://doi.org/10.3390/jcm9072174.

[10] Y. Grossmann, M. Pasciuta, I.M. Finger, A novel technique using a coded healing abutment for the fabrication of a CAD/CAM titanium abutment for an implant-supported restoration, J. Prosthet. Dent. 95 (2006) 258–261, https://doi.org/10.1016/j.prosdent.2005.12.013.

[11] N. Nayyar, B. Yilmaz, E. McGlumphy, Using digitally coded healing abutments and an intraoral scanner to fabricate implant-supported, cement-retained restorations, J. Prosthet. Dent. 109 (2013) 210–215, https://doi.org/10.1016/S0022-3913(13)00073-5.

[12] J. Abduo, C. Chen, E.Le Breton, A. Radu, J. Szeto, R. Judge, I. Darby, The effect of coded healing abutments on treatment duration and clinical outcome: a randomized controlled clinical trial comparing encode and conventional impression protocols, Int. J. Oral. Maxillofac. Implant. 32 (2017) 1172–1179, https://doi.org/10.11607/jomi.5386.M.

[13] B. Yilmaz, S. Abou-Ayash, A digital intraoral implant scan technique using a combined healing abutment and scan body system, J. Prosthet. Dent. 123 (2020) 206–209, https://doi.org/10.1016/j.prosdent.2019.01.016.

[14] Neoss Implant System Website. https://resources.neoss.com/uploads/11926_3-IFU Esthetic- Healing-Abutments-with-ScanPeg-EN-spread-PRINTINT. pdf?mtime=20210330102135. Accessed April 14, 2021.

[15] International Organization for Standardization. Accuracy, (Trueness and Precision) of Measurement Methods and Results e Part 1: General Principles and Definitions (ISO 5725e1:1994), Beuth Verlag GmbH, Berlin, 1997.

[16] A. Ender, A. Mehl, Accuracy of complete-arch dental impressions: a new method of measuring trueness and precision, J. Prosthet. Dent. 109 (2013) 121–128, https://doi.org/10.1016/S0022-3913(13)60028-1.

[17] S. Logozzo, E.M. Zanetti, G. Franceschini, A. Kilpelä, A. Mäkynen, Recent advances in dental optics – Part I: 3D intraoral scanners for restorative dentistry, Opt. Lasers. Eng. 54 (2014) 203–221. http://doi.org/10.1016/j.optlaseng.2013.07.017.

[18] F.G. Mangano, G. Veronesi, U. Hauschild, E. Mijiritsky, C. Mangano, Trueness and precision of four intraoral scanners in oral implantology: a comparative in vitro study, PLoS ONE 11 (2016), e0163107, https://doi.org/10.1371/journal.pone.0163107.

[19] B. Yilmaz, D. Gouveia, V.R. Marques, E. Diker, M. Schimmel, S. Abou-Ayash, The accuracy of single implant scans with a healing abutment-scanpeg system compared with the scans of a scanbody and conventional impressions: an in vitro study, J. Dent. 110 (2021), 103684, https://doi.org/10.1016/j.jdent.2021.103684.

[20] The Sirona web site, https://manuals.sirona.com/en/digital-dentistry/cerec-chairsidesolutions/cerec-omnicam-ac accessed on 21.04.2021.

[21] The Sirona web site, https://manuals.sirona.com/en/digital-dentistry/cerec-chairsidesolutions/cerec-primescan-ac accessed on 21.04.2021.

[22] The 3Shape Web Site https://3shape.widen.net/view/pdf/xt7bnel76t/TRIOS-UserManual- 2015-1-1.4.7.0-A-EN.pdf?t.download=true&u=6xmdhr accessed on 21.04.2021.

[23] R.J.Y. Kim, G.I. Benic, J.M. Park, Trueness of ten intraoral scanners in determining the positions of simulated implant scan bodies, Sci. Rep. 11 (2021) 2606, https://doi.org/10.1038/s41598-021-82218-z.

[24] T. Jemt, Failures and complications in 391 consecutively inserted fixed prostheses supported by Brånemark implants in edentulous jaws: a study of treatment from the time of prosthesis placement to the first annual checkup, Int. J. Oral Maxillofac. Implants. 6 (1991) 270–276.

[25] S.L. Imburgia, U. Hauschild, G. Veronesi, C. Mangano, F.G. Mangano, Accuracy of four intraoral scanners in oral implantology: a comparative in vitro study, BMC Oral Health 17 (2017) 92, https://doi.org/10.1186/s12903-017-0383-4.

[26] G. Revell, B. Simon, A. Mennito, Z.P. Evans, M.L. W.Renne, J. Vág, Evaluation of complete-arch implant scanning with 5 different intraoral scanners in terms of trueness and operator experience, J. Prosthet. Dent. (2021), https://doi.org/10.1016/j.prosdent.2021.01.013 online ahead of print.

[27] Y. Memari, M. Mohajerfar, A. Armin, F. Kamalian, V. Rezayani, E. Beyabanaki, Marginal adaptation of CAD/CAM all-ceramic crowns made by different impression methods: a literature review, J. Prosthodont. 28 (2019) e536–e544, https://doi.org/10.1111/jopr.12800.

[28] A. Schmidt, J.W. Billig, M.A. Schlenz, P. Rehmann, B. Wöstmann, Influence of the accuracy of intraoral scanbodies on implant position: differences in manufacturing tolerances, Int. J. Prosthodont. 32 (2019) 430–432, https://doi.org/10.11607/ijp.6371.

[29] H. Lerner, K. Nagy, F. Luongo, G. Luongo, O. Admakin, F.G. Mangano, Tolerances in the production of six different implant scanbodies: a comparative study, Int. J. Prosthodont. (2021), https://doi.org/10.11607/ijp.7379 online ahead of print.

[30] A. Schmidt, C.R. Benedickt, M.A. Schlenz, P. Rehmann, B. Wöstmann, Torsion and linear accuracy in intraoral scans obtained with different scanning principles, J. Prosthodont. Res. 64 (2020) 167–174, https://doi.org/10.1016/j.jpor.2019.06.006.

[31] B. Giménez, M. Özcan, F. Martínez-Rus, G. Pradíes, Accuracy of a digital impression system based on parallel confocal laser technology for implants with consideration of operator experience and implant angulation and depth, Int. J. Oral Maxillofac. Implants. 29 (2014) 853–862, https://doi.org/10.11607/jomi.3343.

[32] B. Giménez, M. Özcan, F. Martínez-Rus, G. Pradíes, Accuracy of a digital impression system based on active triangulation technology with blue light for implants: effect of clinically relevant parameters, Implant Dent 24 (2015) 498–504, https://doi.org/10.1097/ID.0000000000000283.